Official Journal of Erciyes University Faculty of Medicine

DOI: 10.14744/cpr.2026.48521
J Clin Pract Res 2026;48(4):453–459

Comparison of the Diagnostic Efficacy of Frameless Stereotactic Biopsy (Varioguide) with Other Methods Reported in the Literature: A Single-Center Experience

Halil Ulutabanca,[1] Mehmet Berat Erturhan,[1] Ahmet Küçük,[1] Şükrü Oral,[1] Ali Şahin,[1] Nimetullah Alper Durmuş,[1] Aykut İlikhan[2]

[1]Department of Neurosurgery, Faculty of Medicine, Erciyes University, Kayseri, Türkiye
[2]Department of Neurosurgery, Kayseri City Hospital, Kayseri, Türkiye

ABSTRACT

Objective: To evaluate the diagnostic yield, complication profile, and demographic and radiological factors associated with procedural success in intracranial biopsies performed using the VarioGuide frameless stereotactic system.

Materials and Methods: We retrospectively reviewed 58 consecutive patients who underwent VarioGuide-assisted frameless stereotactic brain biopsy between August 2018 and December 2025. All procedures were performed under general anesthesia using co-registered preoperative high-resolution computed tomography and magnetic resonance imaging datasets. The associations of age, sex, lesion volume, and contrast-enhancement pattern with diagnostic success and postoperative complications were evaluated using exploratory univariable analyses.

Results: The cohort included 42 male (72.4%) and 16 female (27.6%) patients, with a mean age of 49.8±18.7 years. The diagnostic yield was 94.8% (55/58). The median age was 51 years (range, 6–79 years) among patients with diagnostic biopsies and 28 years (range, 2–41 years) among those with non-diagnostic biopsies (exact Mann–Whitney U test, p=0.020). Lesion volume (p=0.843), sex (p=0.181), and contrast-enhancement pattern (p>0.999) were not significantly associated with diagnostic success. Postoperative findings occurred in 10 patients (17.2%), including asymptomatic microhemorrhage in six (10.3%), pneumocephalus in two (3.4%), and symptomatic hematomas requiring surgical decompression in two (3.4%). Neither age (p=0.133) nor lesion volume (p=0.951) differed significantly according to complication status.

Conclusion: In this retrospective single-center series, VarioGuide-assisted frameless stereotactic biopsy provided a high diagnostic yield and a low rate of major procedure-related morbidity. Younger age was associated with a non-diagnostic biopsy in an exploratory analysis; however, this finding should be interpreted cautiously because only three biopsies were non-diagnostic.

Keywords: Associated factors, brain biopsy, complications, diagnostic yield, frameless stereotaxy, varioguide.

Cite this article as:
Ulutabanca H, Erturhan MB, Küçük A, Oral Ş, Şahin A, Durmuş NA, İlikhan A. Comparison of the Diagnostic Efficacy of Frameless Stereotactic Biopsy (Varioguide) with Other Methods Reported in the Literature: A Single-Center Experience. JClinPractRes2026;48(4):453–459.

Address for correspondence:
Halil Ulutabanca.
Department of Neurosurgery, Faculty of Medicine, Erciyes University, Kayseri, Türkiye
Phone: +90 507 755 38 18
E-mail:
ulutabanca@erciyes.edu.tr

Submitted: 20.05.2026
Revised: 26.07.2026
Accepted: 30.07.2026
Available Online: 17.08.2026

Erciyes University Faculty of Medicine Publications - Available online at www.jcpres.com

INTRODUCTION

In the management of intracranial lesions, establishing a definitive histopathological diagnosis is the gold standard for determining the optimal treatment strategy.[1,2] Stereotactic biopsy plays a critical role, particularly in the diagnosis of lesions that are deeply located, adjacent to eloquent areas, multiple, or unsuitable for surgical resection.[3] Conventional frame-based stereotactic systems, which have been used for many years with high accuracy, have disadvantages such as patient discomfort caused by the rigid frame, logistical challenges between preoperative imaging and surgery, and prolonged operative times.[4,5] Frameless neuronavigation systems developed to overcome these limitations have gained an important role in clinical practice.[6,7] Systems such as VarioGuide (Brainlab, Munich, Germany) may streamline the operative workflow and allow more flexible use of preoperative imaging.[8] Frameless systems have been reported to provide diagnostic yields and accuracy rates comparable to those of frame-based systems.[9,10] This retrospective study aimed to evaluate the diagnostic yield, postoperative morbidity, and demographic and radiological factors associated with diagnostic success and complications in a single-center series of VarioGuide-assisted frameless stereotactic biopsies.

KEY MESSAGES

- In this retrospective single-center series of 58 patients, VarioGuide-assisted frameless stereotactic biopsy achieved a diagnostic yield of 94.8% (55/58).
- Younger age was associated with a non-diagnostic biopsy in an exploratory comparison, whereas lesion volume, sex, and contrast-enhancement pattern were not significantly associated with diagnostic success; however, this finding should be interpreted cautiously because only three biopsies were non-diagnostic.
- Procedure-related complications occurred in 17.2% of patients and were predominantly minor and asymptomatic; major hematomas requiring surgical decompression occurred in 3.4%, and no procedure-related mortality was observed.

MATERIALS AND METHODS

Study Site, Design, and Study Period

This retrospective, single-center clinical study was conducted at Erciyes University. We retrospectively reviewed all consecutive patients who underwent frameless stereotactic brain biopsy using the VarioGuide system (Brainlab, Munich, Germany) between August 2018 and December 2025. The study was designed to evaluate diagnostic yield, surgical morbidity, complication profiles, and demographic and radiological factors associated with procedural success.

Ethics Approval

The study was approved by Erciyes University Clinical Research Ethics Committee (Approval Number: 2026/211, Date: 22.04.2026) and was conducted in accordance with the Declaration of Helsinki.

Sample Size

No a priori sample size calculation was performed because this was a retrospective consecutive case series. All patients who met the eligibility criteria during the predefined study period were included. Because the numbers of non-diagnostic biopsies and postoperative complications were small, the comparative analyses were considered exploratory.

Patients and Data Collection

Demographic information, preoperative radiological examinations, surgical notes, early postoperative CT images, and definitive histopathology reports were obtained from the hospital automation system. Patient age, sex, lesion volume, lesion location, contrast-enhancement pattern, histopathological diagnosis, diagnostic success, and postoperative complications were recorded for analysis.

Diagnostic Criteria

The final diagnosis was based on the histopathological examination of the biopsy specimens. Diagnostic success was defined as the acquisition of sufficient tissue to establish a definitive histopathological diagnosis. Diagnostic yield was calculated as the proportion of patients in whom a definitive histopathological diagnosis was obtained among all patients who underwent biopsy.

Definitions

Lesion location was categorized according to the main anatomical region involved. Contrast enhancement on preoperative MRI was classified as homogeneous, heterogeneous, or absent. Lesion volume was assessed preoperatively using the navigation and planning software and recorded in cubic centimeters (cm^3). Postoperative complications were evaluated using early postoperative CT findings and clinical records. Major morbidity was defined as a symptomatic hematoma requiring surgical decompression. A non-diagnostic biopsy was defined as failure to establish a definitive histopathological diagnosis after the biopsy procedure.

Inclusion Criteria

Patients were included if they required tissue diagnosis of an intracranial mass, were considered unsuitable for surgical

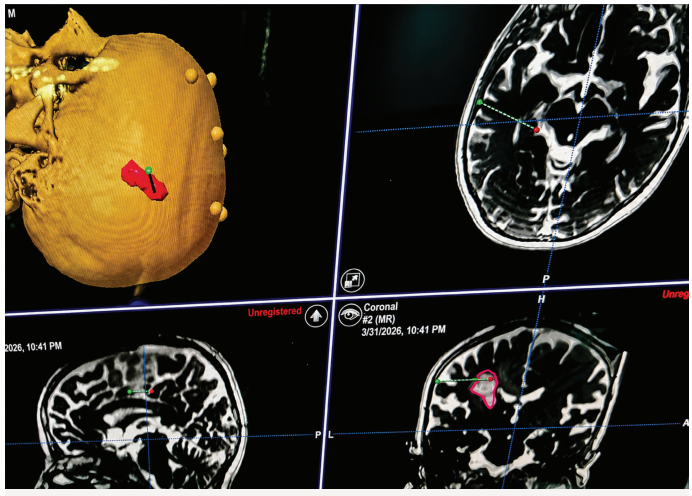

Figure 1. Preoperative planning of a thalamic lesion using neuronavigation software. The target and entry points determined after CT/MRI fusion (co-registration) are shown in the axial, coronal, and sagittal planes. In the three-dimensional reconstruction model in the upper-left panel, the projection of the lesion (red) onto the cranial anatomy and the safest planned surgical trajectory (green line) toward the target are shown.

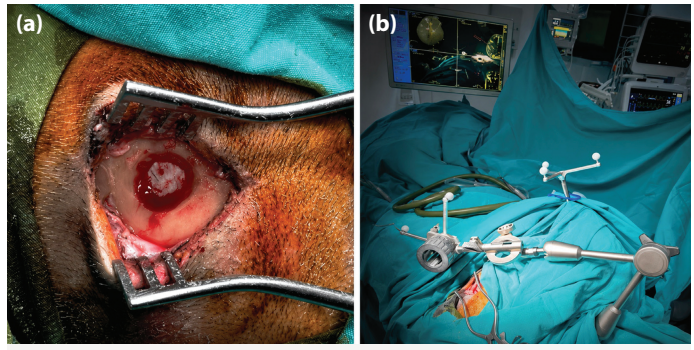

Figure 2. Intraoperative surgical setup and view of the VarioGuide system. **(a)** Macroscopic view of the single burr hole and dural opening created at the planned entry point. **(b)** Operating room setup and integration of the navigation system. The patient's head is secured in a Mayfield skull clamp, and the optical reference stars are registered with the system. The VarioGuide arm (lower center) is integrated into the navigation system and locked along the predetermined surgical trajectory. The optical camera and navigation screen, which provide real-time tracking during the procedure, are visible in the background.

resection because the lesion was deeply located, adjacent to eloquent areas, or multiple, and underwent biopsy using the VarioGuide frameless stereotactic system. Patients with available preoperative MRI/CT data, postoperative CT imaging, surgical records, and histopathological follow-up were included in the analysis.

Exclusion Criteria

Patients whose complete datasets, including preoperative MRI/CT and postoperative CT images, could not be accessed were excluded. Patients with severe coagulopathy or whose antiplatelet or anticoagulant therapy could not be discontinued within a safe period before surgery were also excluded. In addition, cases in which the acceptable registration error margin of 2 mm was exceeded during surgery and cases with incomplete histopathological follow-up were excluded from the evaluation.

Clinical, Surgical, and Laboratory Examinations

All patients underwent preoperative clinical and radiological evaluations. Preoperative magnetic resonance imaging (MRI), including thin-slice contrast-enhanced T1-weighted and T2/FLAIR sequences, was performed. For surgical planning, volumetric computed tomography (CT) suitable for the navigation protocol was obtained. The CT images were transferred to the navigation planning software (Brainlab Elements/iPlan, Brainlab AG) and fused (co-registered) with the preoperative MR images. Using the fused images, the lesion target and entry points were determined, and the safest surgical trajectory that avoided vascular structures, sulci, and ventricles was planned (Fig. 1). Patients underwent routine preoperative laboratory testing, and those with severe coagulopathy were excluded from the study.

All procedures were routinely performed under general anesthesia. The patient's head was secured in a Mayfield pin head-holder system with an integrated navigation reference star. The optical camera system was positioned, and patient registration was completed using anatomical landmarks and surface matching. After registration accuracy was confirmed, the VarioGuide arm was integrated into the navigation system, and instrument calibration was performed (Fig. 2). A linear skin incision was made, followed by the creation of a single burr hole at the planned entry point. After the dura mater was coagulated and incised, the VarioGuide arm was locked along the preplanned trajectory. A Sedan-type biopsy needle was advanced under navigation guidance to the predetermined target depth, and serial samples were obtained from different quadrants through the needle tip (Fig. 3). The samples were sent to the pathology laboratory for histopathological examination. Routine postoperative brain CT was performed in all patients to rule out complications such as hemorrhage or pneumocephalus.

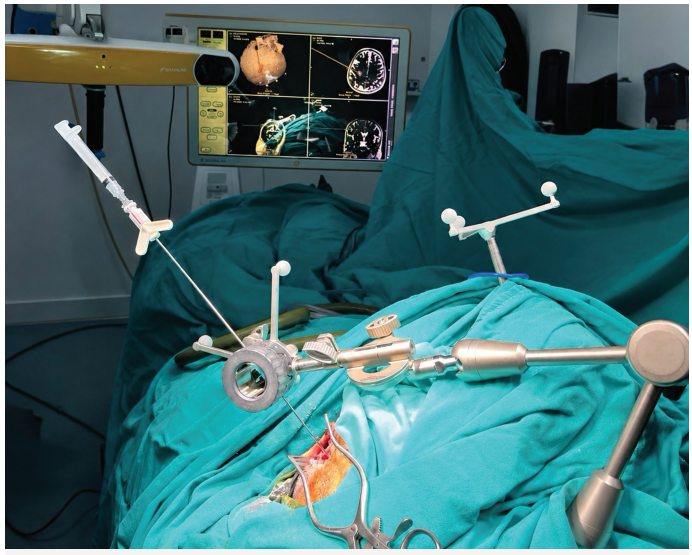

Figure 3. Intraoperative biopsy and tissue sampling. The calibrated Sedan-type stereotactic biopsy needle is advanced to the preplanned target depth in the thalamus under VarioGuide guidance. The image shows the needle being directed toward the intracranial target along the fixed trajectory established by the navigation system. Tissue sampling is performed while monitoring the real-time position of the needle tip and its distance from the target on the navigation screen in the background.

Statistical Analysis

Statistical analyses were performed using IBM SPSS Statistics for Windows, version 25.0 (IBM Corp., Armonk, NY, USA). Continuous variables were summarized as the mean±standard deviation or median (minimum–maximum), as appropriate, and categorical variables were summarized as frequencies and percentages. Age and lesion volume were compared between two independent groups using the two-sided Mann–Whitney U test; exact significance values were used in analyses of diagnostic success because the non-diagnostic group included only three patients. Categorical variables were compared using Fisher's exact test for 2×2 tables and the Fisher–Freeman–Halton exact test for larger contingency tables. Anatomical location was summarized descriptively and was not analyzed inferentially because only three non-diagnostic events were distributed across eight location categories. No adjustment was made for multiple comparisons. A two-sided p value of <0.05 was considered statistically significant.

RESULTS

Demographic and Clinical Characteristics

Of the 58 patients included in the study, 42 were male (72.4%) and 16 were female (27.6%). The mean age of the cohort was 49.81±18.67 years (range, 2–79 years). Radiological evaluation showed a mean lesion volume of 15.12±15.39 cm^3 (range, 1–62 cm^3). Heterogeneous contrast enhancement was observed in 27 lesions (46.6%), homogeneous enhancement in seven (12.1%), and no contrast enhancement in 24 (41.4%) (Table 1).

Table 1. Demographic, clinical, and radiological characteristics of the study population

Variable	n (%) / Mean±SD
Sex	
Male	42 (72.4)
Female	16 (27.6)
Age (years)	
Mean±SD	49.81±18.67
Minimum–maximum	2–79
Lesion location	
Frontal	15 (25.9)
Thalamic	13 (22.4)
Temporal	13 (22.4)
Parietal	12 (20.7)
Occipital	2 (3.4)
Pineal	1 (1.7)
Mesencephalic	1 (1.7)
Intraventricular	1 (1.7)
Contrast enhancement	
Heterogeneous	27 (46.6)
None	24 (41.4)
Homogeneous	7 (12.1)
Lesion volume (cm^3)	
Mean±SD	15.12±15.39

Data are presented as number (percentage) for categorical variables and mean±standard deviation for continuous variables. cm^3, cubic centimeters; n, number of patients; SD: Standard deviation.

The most common lesion location was the frontal lobe (n=15, 25.9%), followed by the thalamus (n=13, 22.4%), temporal lobe (n=13, 22.4%), and parietal lobe (n=12, 20.7%). The remaining lesions were located in the occipital lobe (n=2, 3.4%), mesencephalon (n=1, 1.7%), pineal region (n=1, 1.7%), and lateral ventricle (n=1, 1.7%) (Table 1).

Histopathological Diagnoses

Histopathological analysis revealed diffuse astrocytoma as the most common diagnosis (n=15, 25.9%), followed by high-grade glial tumors (n=10, 17.2%), low-grade glial tumors (n=6, 10.3%), and glioblastoma (n=6, 10.3%). B-cell lymphoma (n=5, 8.6%) and oligodendroglioma (n=5, 8.6%) were also identified.

Table 2. Factors associated with diagnostic success

Variable	Diagnostic biopsy (n=55)	Non-diagnostic biopsy (n=3)	Statistical test	p
Age, years, median (minimum–maximum)	51 (6–79)	28 (2–41)	Exact Mann–Whitney U test	0.020
Lesion volume, cm^3, median (minimum–maximum)	9 (1–62)	7 (6–28)	Exact Mann–Whitney U test	0.843
Sex, n (%)			Fisher's exact test	0.181
Male	41 (74.5)	1 (33.3)		
Female	14 (25.5)	2 (66.7)		
Contrast enhancement, n (%)			Fisher–Freeman–Halton exact test	>0.999
None	23 (41.8)	1 (33.3)		
Heterogeneous	25 (45.5)	2 (66.7)		
Homogeneous	7 (12.7)	0 (0.0)		

Data are presented as median (minimum–maximum) or n (%). Exact two-sided p values were used where indicated. Anatomical location was summarized descriptively and was not analyzed inferentially because only three non-diagnostic events were distributed across eight location categories. cm^3, cubic centimeters; n, number of patients; p, probability value.

Table 3. Factors associated with postoperative complications

Variable	Complication (n=10)	No complication (n=48)	Statistical test	p
Age, years, median (minimum–maximum)	65 (28–79)	48 (2–76)	Mann–Whitney U test	0.133
Lesion volume, cm^3, median (minimum–maximum)	14.5 (2–28)	8.5 (1–62)	Mann–Whitney U test	0.951

Data are presented as median (minimum–maximum). p values were calculated using two-sided Mann–Whitney U tests. cm^3, cubic centimeters; n, number of patients; p, probability value.

Diagnostic Yield and Associated Factors

The overall diagnostic yield was 94.8% (55/58), with three biopsies being non-diagnostic. Two of the non-diagnostic lesions were located in the frontal lobe, and one was located in the temporal lobe. Anatomical location was summarized descriptively and was not subjected to inferential testing because only three non-diagnostic events were distributed across eight location categories.

Patients with diagnostic biopsies had a median age of 51 years (range, 6–79 years), compared with 28 years (range, 2–41 years) among patients with non-diagnostic biopsies (exact Mann–Whitney U test, p=0.020). The median lesion volume was 9 cm^3 (range, 1–62 cm^3) in the diagnostic group and 7 cm^3 (range, 6–28 cm^3) in the non-diagnostic group (p=0.843). Diagnostic success was not significantly associated with sex (Fisher's exact test, p=0.181) or contrast-enhancement pattern (Fisher–Freeman–Halton exact test, p>0.999). Because there were only three non-diagnostic cases, these comparisons were interpreted as exploratory (Table 2).

Surgical Complications and Associated Factors

Procedure-related postoperative findings were recorded in 10 patients (17.2%), including asymptomatic microhemorrhage in six (10.3%), pneumocephalus in two (3.4%), and symptomatic hematoma requiring surgical decompression in two (3.4%). No procedure-related mortality occurred.

The median age was 65 years (range, 28–79 years) among patients with complications and 48 years (range, 2–76 years) among those without complications (Mann–Whitney U test, p=0.133). The median lesion volumes were 14.5 cm^3 (range, 2–28 cm^3) and 8.5 cm^3 (range, 1–62 cm^3), respectively (p=0.951) (Table 3).

DISCUSSION

Histopathological diagnosis remains central to selecting appropriate oncological and surgical treatments for intracranial lesions. In this retrospective series of 58 VarioGuide-assisted frameless stereotactic biopsies, the overall diagnostic yield was 94.8%. This result is within the 91%–99% range reported in contemporary frameless and frame-based stereotactic biopsy series and supports the clinical utility of frameless navigation-guided biopsy systems.[9–12]

In exploratory analyses, younger age was associated with a non-diagnostic biopsy. However, only three non-diagnostic procedures occurred, and this finding should not be interpreted as an established risk factor. Lesion volume, sex,

and contrast-enhancement pattern were not significantly associated with diagnostic success. The three non-diagnostic lesions were located in the frontal (n=2) and temporal (n=1) regions; therefore, lesion location was reported descriptively rather than analyzed inferentially. Larger multicenter series are required to determine whether age or lesion location independently influences diagnostic yield.

Postoperative hemorrhage is the most feared complication of stereotactic brain biopsy and directly contributes to surgical morbidity. In the literature, asymptomatic microhemorrhages have been reported at rates of up to 10%, whereas symptomatic hematomas have been reported at rates ranging from 1% to 6%.[13,14]

Although postoperative findings were recorded in 17.2% of patients, most consisted of asymptomatic microhemorrhages (n=6, 10.3%) or pneumocephalus (n=2, 3.4%) without clinical deficits. Symptomatic hematomas requiring surgical decompression occurred in two patients (3.4%), and no procedure-related mortality was observed. These findings are consistent with the reported morbidity profile of stereotactic brain biopsy.[14,15]

The absence of procedure-related mortality and the low number of major complications support an acceptable safety profile in this cohort. Nevertheless, the absence of statistically significant associations should not be interpreted as evidence that age or lesion volume has no effect because only 10 postoperative events were available for comparison.[15]

The literature suggests that necrotic or fragile vascular structures in very large lesions or multiple needle passes required to reach the target in very small lesions may increase the risk of bleeding.[16]

In our cohort, age and lesion volume did not differ significantly between patients with and without postoperative complications (p=0.133 and p=0.951, respectively). These exploratory comparisons suggest that no clear association was detectable in the present sample; however, the limited number of events reduced statistical power and precluded reliable multivariable modeling.

One of the most common criticisms of frameless systems is the risk of missing the target, particularly in very small or non-enhancing lesions.[17,18]

Diagnostic success was not significantly associated with lesion volume (p=0.843) or contrast-enhancement pattern (p>0.999). Twenty-four lesions (41.4%) showed no contrast enhancement, and the overall diagnostic yield remained high. These observations suggest that VarioGuide-assisted biopsy may be clinically useful across heterogeneous radiological presentations; however, they do not establish equivalent performance across lesion subgroups because the non-diagnostic group was very small.

Limitations

This study has several limitations. Its retrospective, single-center design may introduce selection and information biases and limit generalizability. No a priori power calculation was performed because all eligible consecutive patients were included. The small numbers of non-diagnostic biopsies (n=3) and postoperative complications (n=10) limited statistical power, precluded reliable multivariable modeling, and increased the possibility of unstable estimates. Therefore, the observed association between younger age and a non-diagnostic biopsy should be considered exploratory and requires confirmation in larger cohorts. In addition, variables such as lesion consistency, the number of tissue samples, and minor differences in surgical technique could not be quantitatively evaluated.

CONCLUSION

In this retrospective single-center series, VarioGuide-assisted frameless stereotactic biopsy provided a high diagnostic yield and a low rate of major procedure-related morbidity. Younger age was associated with a non-diagnostic biopsy in an exploratory analysis, whereas lesion volume, sex, and contrast-enhancement pattern were not significantly associated with diagnostic success. These findings support the clinical utility of the system but should be interpreted cautiously because of the small number of non-diagnostic cases.

Ethics Committee Approval: Ethics committee approval was obtained from Erciyes University Clinical Research Ethics Committee (Approval Number: 2026/211, Date: 22.04.2026).

Informed Consent: Informed consent was waived due to the retrospective nature of the study.

Conflict of Interest: The authors have no conflicts of interest to declare.

Financial Disclosure: The authors declared that this study received no financial support.

Use of AI for Writing Assistance: No use of AI-assisted technologies was declared by the authors.

Author Contributions: Concept – HU, MBE; Design – HU, MBE; Supervision – HU, Aİ; Resources – HU, AK; Materials – ŞO, AŞ, NAD; Data Collection and/or Processing – HU, MBE, AK; Analysis and/or Interpretation – MBE, HU, Aİ; Literature Review – MBE, HU; Writing – MBE, HU; Critical Review – HU, Aİ, AK, ŞO, AŞ, NAD.

Peer-review: Externally peer-reviewed.

REFERENCES

1. Bradac O, Steklacova A, Nebrenska K, Vrana J, de Lacy P, Benes V. Accuracy of VarioGuide Frameless Stereotactic System Against Frame-Based Stereotaxy: Prospective, Randomized, Single-Center Study. World Neurosurg 2017;104:831-40. [CrossRef]
2. Hall WA. The safety and efficacy of stereotactic biopsy for intracranial lesions. Cancer 1998;82(9):1749-55. [CrossRef]
3. Akshulakov SK, Kerimbayev TT, Biryuchkov MY, Urunbayev YA, Farhadi DS, Byvaltsev VA. Current Trends for Improving Safety of Stereotactic Brain Biopsies: Advanced Optical Methods for Vessel Avoidance and Tumor Detection. Front Oncol 2019;9:947. [CrossRef]
4. Owen CM, Linskey ME. Frame-based stereotaxy in a frameless era: current capabilities, relative role, and the positive- and negative predictive values of blood through the needle. J Neurooncol 2009;93(1):139-49. [CrossRef]
5. Grimm F, Naros G, Gutenberg A, Keric N, Giese A, Gharabaghi A. Blurring the boundaries between frame-based and frameless stereotaxy: feasibility study for brain biopsies performed with the use of a head-mounted robot. J Neurosurg 2015;123(3):737-42. [CrossRef]
6. Moon JH, Kim JS, Chang JW. Frameless stereotactic brain biopsy. J Korean Neurosurg Soc 2021;17(1):64-70.
7. Lim DH, Kim SY, Na YC, Cho JM. Navigation-guided biopsy effectiveness. J Pers Med 2023;13(5):708. [CrossRef]
8. Buchalla R, Hopf-Jensen S, Rubarth O, Börm W. Frameless navigated biopsy with the BrainLAB® VarioGuide system: a technical note. J Neurol Surg A Cent Eur Neurosurg 2013;74(5):321-4. [CrossRef]
9. Ringel F, Ingerl D, Ott S, Meyer B. VarioGuide: a new frameless image-guided stereotactic system--accuracy study and clinical assessment. Neurosurgery 2009;64(5 Suppl 2):365-71; discussion 371-3. [CrossRef]
10. Woodworth G, McGirt MJ, Samdani A, Garonzik I, Olivi A, Weingart JD. Accuracy of frameless and frame-based image-guided stereotactic brain biopsy in the diagnosis of glioma: comparison of biopsy and open resection specimen. Neurol Res 2005;27(4):358-62. [CrossRef]
11. Dammers R, Haitsma IK, Schouten JW, Kros JM, Avezaat CJ, Vincent AJ. Safety and efficacy of frameless and frame-based intracranial biopsy techniques. Acta Neurochir (Wien) 2008;150(1):23-9. [CrossRef]
12. Maciunas RJ, Galloway RL Jr, Latimer JW. The Application Accuracy of Stereotactic Frames. Neurosurgery 1994;35(4):682-95. [CrossRef]
13. Henderson JM, Holloway KL, Gaede SE, Rosenow JM. The application accuracy of a skull-mounted trajectory guide system for image-guided functional neurosurgery. Computer Aided Surgery 2004;9(4):155-60. [CrossRef]
14. Kreth FW, Muacevic A, Medele R, Bise K, Meyer T, Reulen HJ. The risk of haemorrhage after image guided stereotactic biopsy of intra-axial brain tumours--a prospective study. Acta Neurochir (Wien) 2001;143(6):539-45; discussion 545-6. [CrossRef]
15. Kulkarni AV, Guha A, Lozano A, Bernstein M. Incidence of silent hemorrhage and delayed deterioration after stereotactic brain biopsy. J Neurosurg 1998;89(1):31-5. [CrossRef]
16. Vychopen M, Wach J, Borger V, Schneider M, Eichhorn L, Maciaczyk J, et al. Patient Safety Comparison of Frameless and Frame-Based Stereotactic Navigation for Brain Biopsy-A Single Center Cohort Study. Brain Sci 2022;12(9):1178. [CrossRef]
17. Ungar L, Nachum O, Zibly Z, Wohl A, Harel R, Attia M, et al. Comparison of Frame-Based Versus Frameless Image-Guided Intracranial Stereotactic Brain Biopsy: A Retrospective Analysis of Safety and Efficacy. World Neurosurg 2022;164:e1-7. [CrossRef]
18. Meinert F, Dömer P, Helgers SOA, Tanrikulu L, Woitzik J, Wendt-Thakur N. Accuracy of frameless stereotactic brain biopsy: a retrospective cohort study with MRI-only and MRI-CT fusion navigation. Acta Neurochir (Wien) 2025;167(1):327. [CrossRef]